JOURNAL OF MATERIALS SCIENCE **35** (2000) 2749–2756

Effect of halogen purification and heat treatment on thermal conductivity of high porosity carbon/carbon composite thermal insulation

R. I. BAXTER*, N. IWASHITA, Y. SAWADA
Osaka National Research Institute, AIST, 1-8-31 Midorigaoka, Ikeda, Osaka 563-8577, Japan
E-mail: iwashita@onri.go.jp

Thermal conductivity of a highly porous carbon/carbon composite, known as carbon bonded carbon fiber (CBCF) and used as thermal insulation, was measured and related to the structure investigated by optical microscopy, x-ray diffraction and Raman spectroscopy. It was found that halogen purification of CBCF, that involves heat treatment in chlorine atmosphere, did not result in a greater extent of structural development than heat treatment at the same temperature for the same time in inert atmosphere (unpurified sample). The thermal conductivity of CBCF, both halogen purified and unpurified, was found to increase with temperature in the measured range 1000°C to 2200°C. The experimental thermal conductivity values were in good agreement with those calculated from a model that indicated that in CBCF solid heat transfer was dominant, compared to radiation heat transfer, even at 2200°C. The matrix in CBCF was found to be relatively graphitic as a result of stress orientation on carbonization and as matrix was observed along the fiber length it was tentatively suggested that it may contribute to the effective axial conductivity of the fibers.

1. Introduction

High porosity carbon/carbon composites, with a density of between 0.1–0.4 Mgm^{-3}, are used as insulation in furnaces at temperatures up to 2800°C. They consist of a carbon fiber network bonded together at the intersections of the fibers by discrete regions of carbon matrix, hence they are also known as carbon-bonded carbon fiber (CBCF). The vast majority of the volume (70–90%) consists of interconnected pores. A consequence of the vacuum molding process used in composite production is that the discontinuous carbon fibers are orientated into layers to form a 2D planar random structure (Fig. 1). The high porosity content and fiber orientation result in a low thermal conductivity perpendicular to the fiber layer arrays (*z*-direction), hence their use as furnace insulation [1]. Investigations into the microstructure [2, 3], mechanical properties [2–8] and thermal properties [9–11] of these materials have been reported.

CBCF is used in furnaces utilized for growing silicon single crystals; these furnaces have a temperature capability of 1600–2000°C and are evacuated or filled with inert gas [12]. The high purity of the growing chamber, and hence the thermal insulation, is important to avoid contamination of the melt leading to faults in the crystals. As shown by neutron activation analysis the impurity content of CBCF insulation is low (less than 0.1%), and it can be further reduced by halogen purification treatments [13]. Different gas atmospheres are known to effect graphitization, possibly by the reaction with cross-links reducing the obstacles that inhibit the structural development [14]. The possibility of the halogen atmosphere affecting the structure of the rayon derived carbon fibers or the phenolic derived matrix in CBCF must be considered. The crystal structure (i.e. degree of graphitization) is an important factor with respect to the thermal conductivity; it is well known for carbon materials that thermal conductivity increases with crystallite size [15, 16]. This paper reports an investigation into the effect of halogen purification and heat treatment on the crystal structure and thermal conductivity of CBCF.

2. Experimental

2.1. Samples

CBCF samples were manufactured by Calcarb Ltd, Bellshill, Scotland, UK by the process illustrated in the schematic flow diagram in Fig. 2. The sample termed 'halogen purified' was subjected to halogen purification under a commercially sensitive process at a temperature of about 2200°C for a period of 6 hours. The sample termed 'unpurified' was heat treated at the same temperature and for the same time but under argon. Further heat treatments of both halogen purified and unpurified samples were carried out at temperatures between

* Author to whom all correspondence should be addressed.

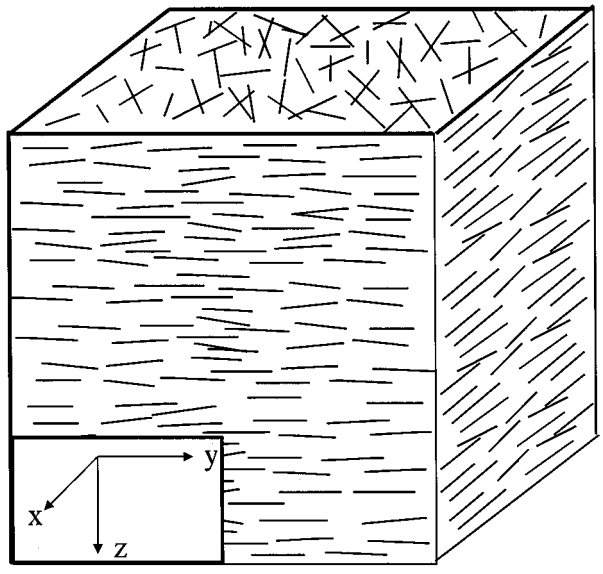

Figure 1 Schematic of the structure of carbon-bonded carbon fiber (CBCF).

2200–3000°C under argon with a residence time at the maximum temperature of 30 minutes.

2.2. Procedure

Thermal diffusivity was obtained on a TC-7000UVH using the laser flash diffusivity method in accordance with ASTM E1461 [17]. In this method the front face of the sample is illuminated with a short laser pulse and the temperature change of the back face is monitored by a pyrometer. For the experiment to be valid for composite materials the material must adhere to the continuum model such that the local discontinuities are small relative to the external dimensions of the composite [18]. Another complication with porous materials is that the laser pulse energy will not impart entirely on the surface but over a region equivalent to the radiation mean free path. Likewise radiation from a distance of up to the radiation mean free path from the bottom surface of the specimen will be collected by

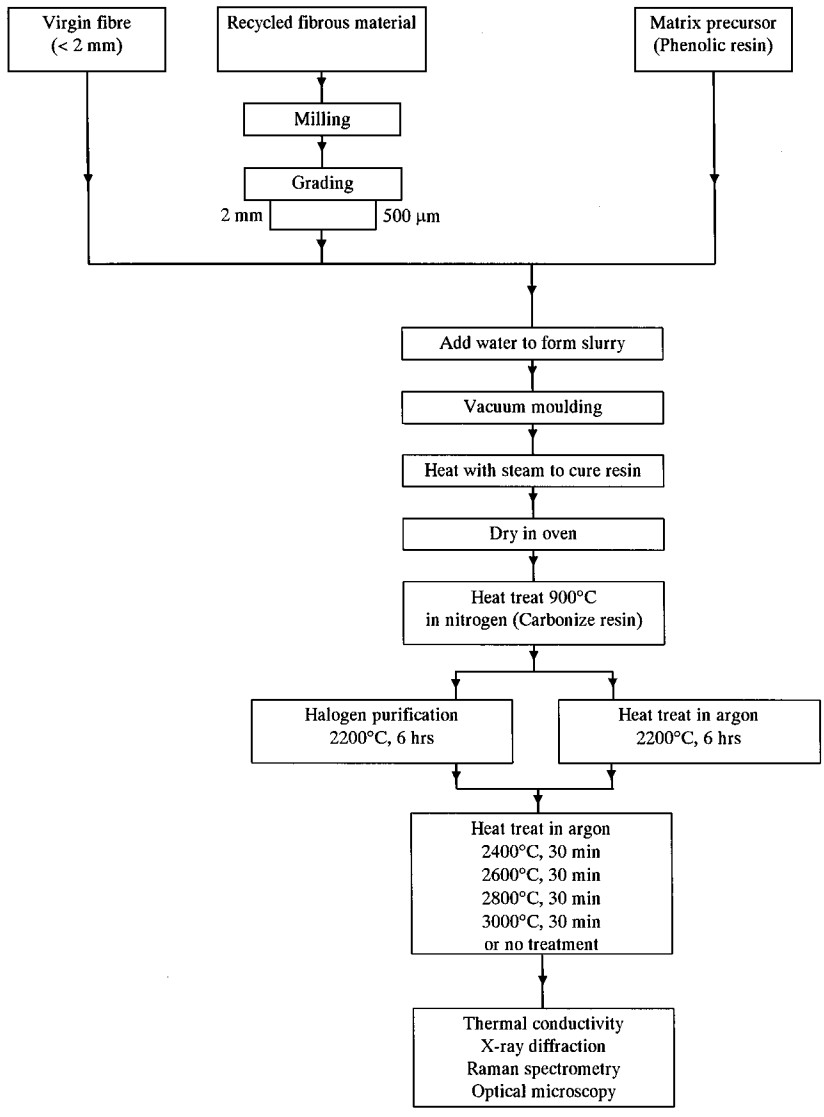

Figure 2 Flow diagram of the production process of CBCF.

the optical pyrometer. In these experiments the maximum values for these distances were estimated to be less than 5% of the thickness of the sample. The measurements were carried out between 1000–2200°C in argon on disk shaped samples with a diameter of 10 mm and a thickness of 1–1.5 mm. Samples were tested both parallel (x and y, but as x and y are equivalent they are referred to as x in the following text) and perpendicular (z) to the fiber array. The results were corrected to account for radiative heat loss effects by the proportioning procedure described by Cowan [19]. The thermal conductivity (K) was calculated from

$$K = \alpha \cdot C_{\mathrm{p}} \cdot \rho \tag{1}$$

where α is the thermal diffusivity (m^2s^{-1}), C_p is the specific heat capacity ($Jg^{-1}K^{-1}$) and ρ is the bulk density (gm^{-3}). The values of specific heat capacity, which increases as a function of temperature, were taken from reference 20.

Powder x-ray diffraction measurements were taken on a Rigaku diffractometer, operated at 40 kV and 150 mA, using Cu K_α radiation (0.15405 nm). The position and widths of the peaks were calibrated with respect to a silicon internal standard. The interlayer spacing and crystallite size were calculated from the Bragg and Scherrer equations, respectively [21].

Raman measurements were taken on polished optical microscopy specimens using an Instruments SA T64000 spectrometer with an argon laser at an excitation wavelength of 514.5 nm. Back-scattered mode was used to obtain first order spectra between 1200–1800 cm^{-1}. In general a $\times 100$ objective was utilized and the spot size was less than 2 μm in diameter. To avoid sample heating effects the laser power was kept below 2 mW at the specimen surface. Calibration of the peak positions was done with respect to highly orientated pyrolytic graphite (HOPG). The deconvolution of the spectra was considered an important aspect and was carried out using 4 Lorentzian peaks in addition to a linear function background in accordance with previous work [22].

3. Results and discussion

Optical micrographs obtained using polarized light, of halogen purified and unpurified samples, are shown in Fig. 3. It should be noted that the majority of the volume of the composite consists of porosity (dark red) and the micrographs shown here are high magnification views of the regions where fibers and matrix are present. The rayon-derived carbon fibers (light red) are about 10 μm in diameter, have a crenulated (celery-like) cross section and are optically isotropic. On the other hand the phenolic resin derived matrix, which mainly exists at fiber intersections, is optically active in all samples and is colored blue or yellow. Phenolic resin is non-graphitizing in the free state, but in the composite it undergoes a structural change on carbonization due to the stresses exerted by the fibers during shrinkage, a phenomenon known as stress orientation [23]. Although it can not be distinguished from optical microscopy, a typical orientation would be that that graphite planes in the matrix are parallel with the fiber surface, so called c-axis radial orientation [23]. This is the first time in the literature that matrix in CBCF has been shown to be optically anisotropic. The appearance of matrix after low and high temperature heat treatment differ. At 3000°C the optically anisotropic areas appear more angular compared with at 2200°C.

Although matrix mainly exists at the intersections of fibers in some instances the matrix is observed along a considerable length of the fiber (Fig. 3e). The coating of fiber and the accumulation of the resin at the intersections of fibers occur when the preform is heated by steam after slurry molding. The solid resin melts, flows down the fiber and accumulates at intersections of fibers as can be seen schematically in Fig. 4. Carbonization of the matrix results in the discrete matrix bonds at the intersection of fibers and it is evident that some of the resin remains on the surface of the fiber along which is flowed.

The interlayer spacing and the crystallite size along the c-axis as a function of heat treatment temperature are shown in Fig. 5a and b, respectively. After consideration of sample variation and experimental error the interlayer spacing and crystallite size along the c-axis are similar for halogen purified and unpurified samples heat treated at 2200°C; hence, under the conditions used here the halogen purification treatment does not result in an increase in graphitisation degree. In addition it can be said that the purification treatment does not result in a carbon that is more amenable to graphitization when subjected to further heat treatment as even after heat treatment at 3000°C the structural parameters of the halogen purified and unpurified samples are similar. For both samples the interlayer spacing is found in the region of 0.342 nm to 0.339 nm where as crystallite size along the c-axis is between 6 nm and 12 nm after heat treatment at temperatures from 2200 °C to 3000°C. These x-ray parameters are more graphitic than would be expected considering the glassy-like structure expected for the rayon-derived fibers that account for about 90% of the weight of the composite. For example a typical glassy-like carbon heat treated at 2500°C was found to have an interlayer spacing and crystallite size along the c-axis of 0.356 nm and 2.4 nm, respectively [24]. The limitation of x-ray diffraction is that it provides an 'average' of the crystallite parameters and not specific information about the phases in the composite. (Note that in fact these values are not a true average as on a weight for weight basis the more highly orientated components produce more intense peaks and therefore dominate the spectrum and the resulting calculated parameters [25].) Examination of the x-ray diffraction spectra shows that the (002) peak, between $2\theta = 20$–30°, is unsymmetrical (Fig. 6). Unsymmetrical peaks often result where the specimen contains several phases with different graphitisation degrees [25]. Consistent with the optical microscopy results, in the next section it will be shown by Raman spectroscopy that the fibers are non-graphitic and the matrix is relatively graphitic. Considering this, it is suggested that the unsymmetrical (002) diffraction peak results from the convolution of the contributions from the

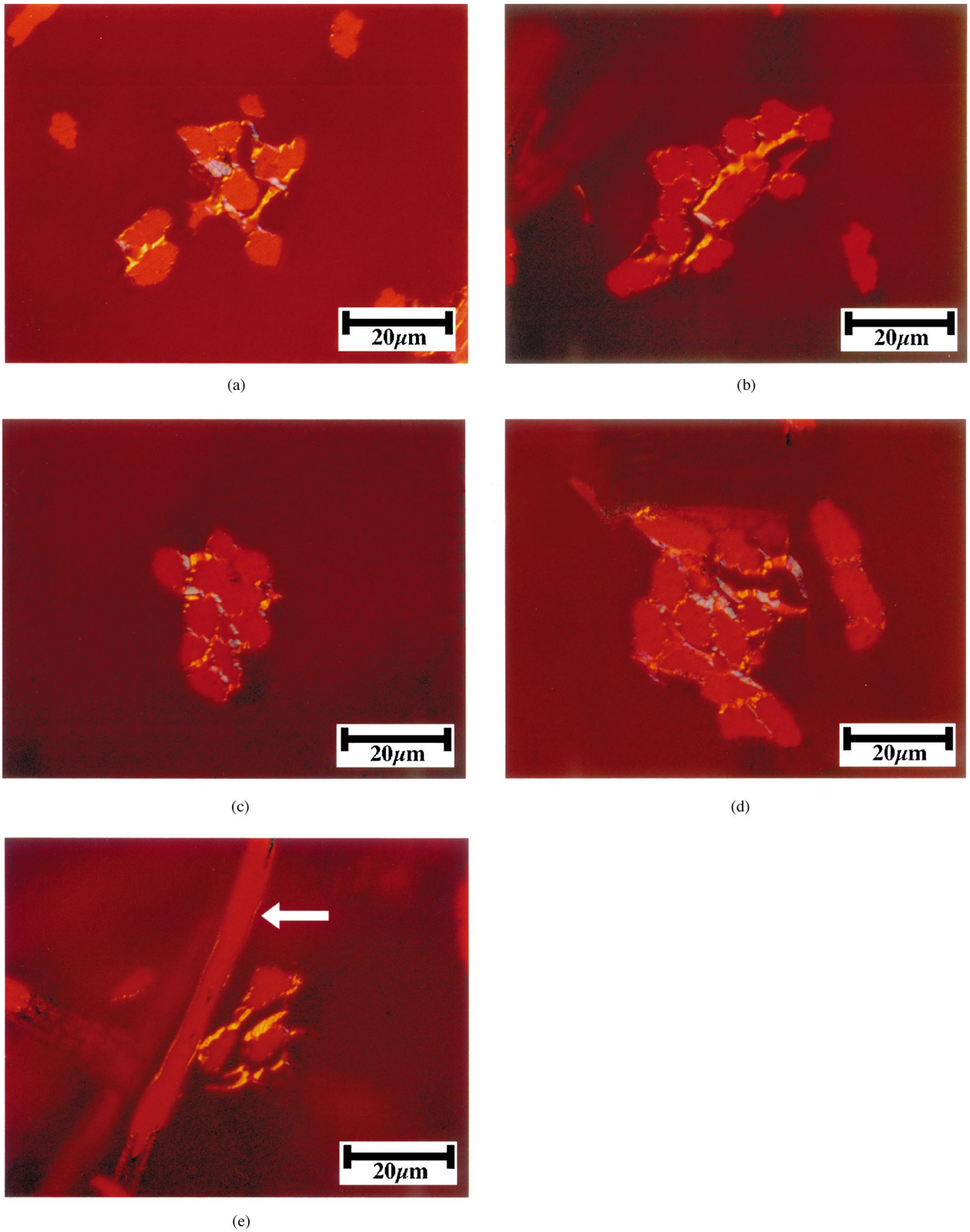

Figure 3 Optical micrograph, using plane polarized light, of halogen purified sample heat treated at (a) 2200°C and (c) 3000°C and unpurified sample heat treated at (b) 2200°C and (d, e) 3000°C. (Carbon fibers—light red, matrix—blue/yellow, porosity—dark red).

non-graphitic fibers and more graphitic matrix. With respect to thermal conductivity a knowledge of the structure of the individual phases is indeed crucial as for fibrous insulation materials it has been proposed that the thermal conductivity of the composite is dependent on that of the fibers and the contribution of the matrix, which is not continuous, is assumed to be insignificant [1, 10, 26, 27].

Information about the structure of the fibers and matrix within the composite can be obtained by micro-Raman spectroscopy. In agreement with x-ray diffraction data, Raman spectra were similar for halogen purified and unpurified samples. Typical peaks for the matrix and fibers in the unpurified composite (polished optical microscopy specimens) heat treated at 2200°C and 3000°C are presented in Fig. 7. For comparison,

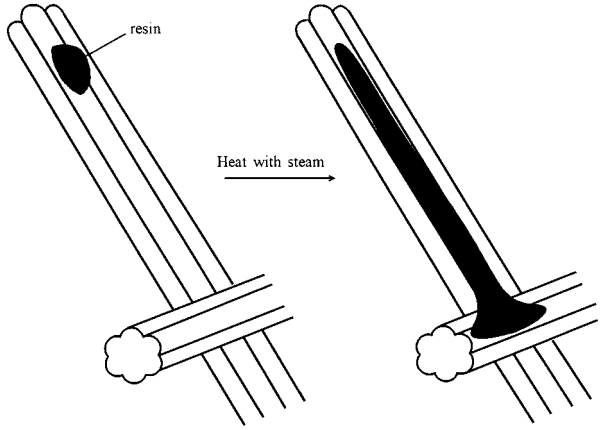

Figure 4 Schematic showing the resin, after heating with steam, flowing down fiber and accumulating at fiber intersections to form discrete matrix bonds.

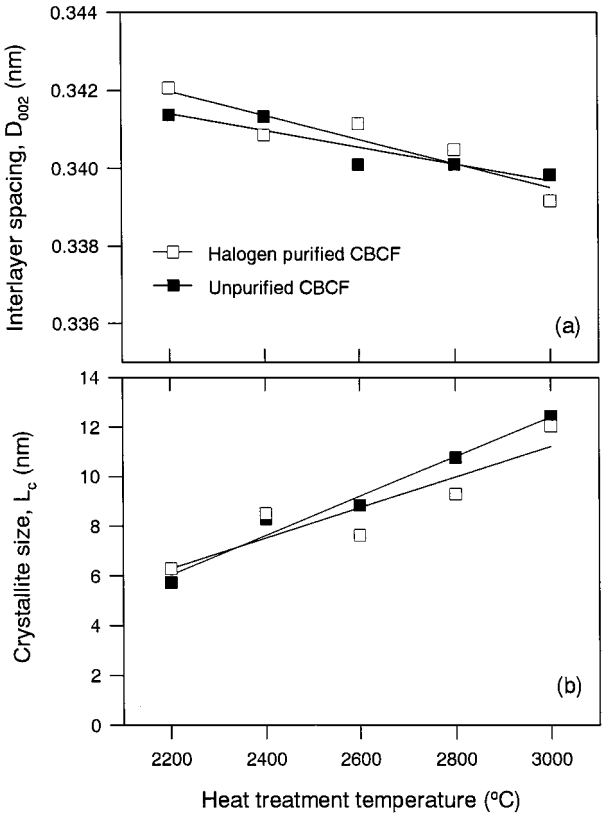

Figure 5 (a) Interlayer spacing and (b) crystallite size along *c*-axis (L_c) as a function of heat treatment temperature for halogen purified and unpurified CBCF.

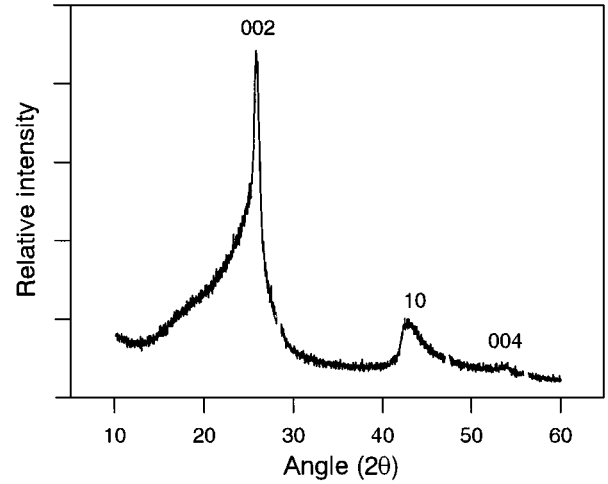

Figure 6 Representative x-ray diffraction spectrum for unpurified CBCF heat treated at 2200°C.

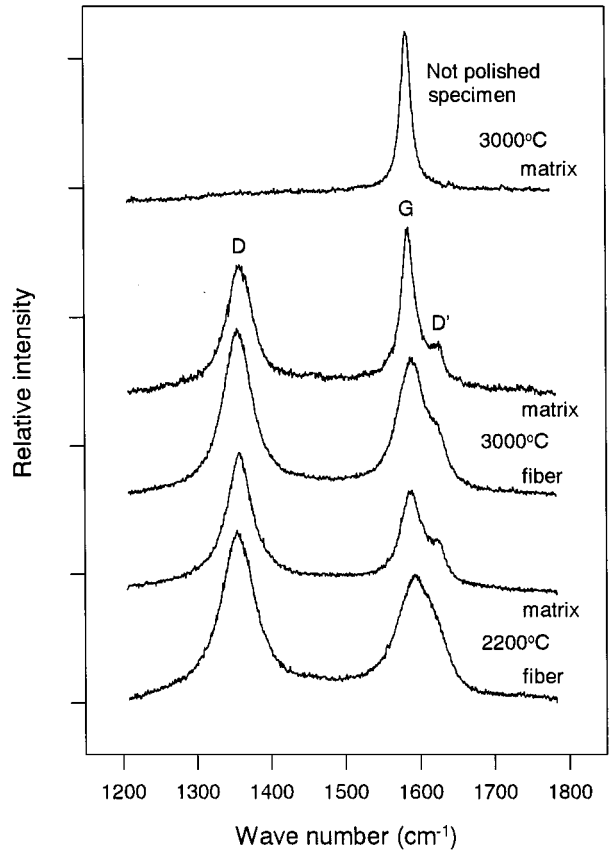

Figure 7 Representative Raman spectra for the fiber and matrix in unpurified CBCF heat treated at 2200°C and 3000°C using polished optical microscopy specimens. For comparison a spectrum taken from matrix in unpurified CBCF heat treated at 3000°C using a non-polished specimen is presented.

to demonstrate the effect of polishing, a spectra taken from matrix in a unpurified composite heat treated at 3000°C which had not been mounted and polished is also shown. Spectra of carbon materials exhibit peaks at approximately 1360 cm^{-1} (D peak) and 1585 cm^{-1} (G peak) in addition to a peak at 1620 cm^{-1} (D" peak) which is evident as a shoulder on the G peak. The G peak is associated with the E_{2g} in-plane vibrational mode of graphite where as the D and D' peaks are associated with disorder in the structure [28]. The polished samples exhibit a much higher D peak intensity, probably due to the disorder induced in the specimen by mechanical polishing. However, on polished samples the areas of fiber and matrix could be clearly distinguished where as on unprepared specimens, although the fiber and matrix present at the fiber intersections were visible, the coating of matrix on the fiber was not resolvable. As Raman spectrum are taken from only a small depth (50 nm) [29] if the laser is positioned on a part of the fiber which has a matrix coating the spectra will arise from matrix but will mistakenly be assigned to fiber. Therefore, for comparison purposes polished samples were used and the position and

TABLE I G peak position and half width at half height obtained from the Raman spectra for fibers and matrix in halogen purified and unpurified CBCF heat treated at 2200°C and 3000°C

Heat treatment temp. (°C)	G peak position (half width at half height in brackets). (cm^{-1})			
	Halogen purified CBCF		Unpurified CBCF	
	Fiber	Matrix	Fiber	Matrix
2200	1590.2 (28.4)	1587.2 (20.6)	1588.8 (28.0)	1586.1 (20.2)
3000	1587.5 (22.0)	1582.4 (9.8)	1586.4 (22.5)	1582.5 (11.0)

width of the G peak, which is relatively unaffected by polishing, were compared. The position and half width at half height of the G peak, which generally decreases with graphitisation degree, for both halogen purified and unpurified composites, heat treated at 2200°C and 3000°C are presented in Table I. The G peak positions and half width at half height can be compared against those of HOPG which are 1582 cm^{-1} and 6 cm^{-1}, respectively [30]. The low G peak position and narrow G peak indicate that the matrix is more graphitic than the fibers. This may be expected considering the results of the optical investigation that showed that the matrix was optically anisotropic. In addition the matrix showed a much greater change towards the graphite structure on heat treatment at 3000°C, this behavior results from the structure of the matrix being rendered graphitizable by "stress orientation". On the other hand, the fibers show a relatively small change in Raman parameters on heat treatment to 3000°C, indicative of their non-graphitizing nature, structural ordering being restrained by the extensive cross-linking [24].

The thermal conductivity of halogen purified and unpurified samples, heat-treated at 2200°C and 3000°C, in the direction parallel (x) and perpendicular (z) to the fiber array are shown in Fig. 8. It is noted that, (i) thermal conductivity increases with temperature, (ii) thermal conductivity is significantly greater parallel (x) compared to the perpendicular (z) to the fiber array, (iii) both halogen purified and unpurified samples show similar values for thermal conductivity which indicates

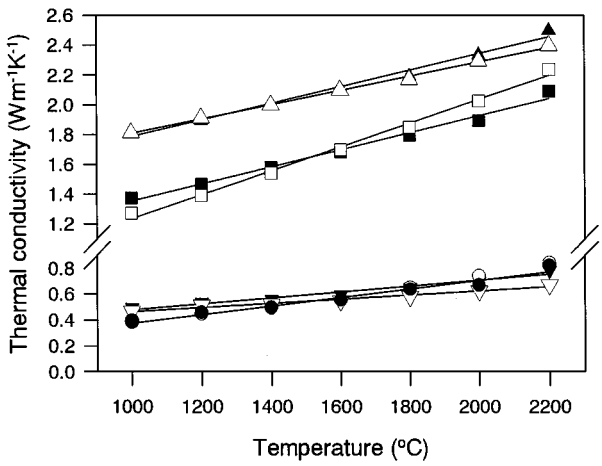

Figure 8 Thermal conductivity as a function of temperature for halogen purified and unpurified CBCF, subjected to a heat treatment at 2200°C and 3000°C, in the x and z-directions. Halogen purified CBCF: (■) x 2200°C; (●) z 2200°C; (▲) x 3000°C; (▼) z 3000°C. Unpurified CBCF: (□) x 2200°C; (○) z 2200°C; (△) x 3000°C; (▽) z 3000°C.

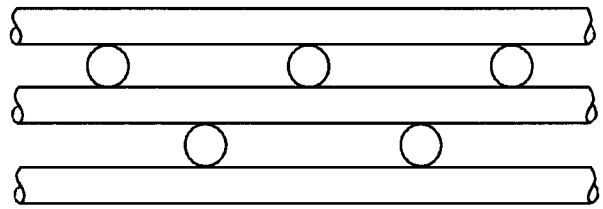

Figure 9 Model fiber arrangement in CBCF.

the purification procedure has little effect on thermal conductivity, (iv) perpendicular to the fiber array (z) samples heat treated at 3000°C have greater thermal conductivity up to a test temperature of 1400°C above which the heat treatment has little effect and, (v) parallel to the fiber array (x) at 1000°C thermal conductivity increases by about 40% on increasing the heat treatment temperature from 2200°C to 3000°C but the effect is lower at higher test temperatures.

For fibrous insulation materials the overall effective thermal conductivity is the sum of contributions from solid heat transfer, radiation heat transfer and, in the non-vacuum case, heat transfer taking a path through the gas present in the pores. Simplified models of the fiber arrangement have been used to calculate the thermal conductivity of fibrous insulation materials [1, 10, 26, 27]. In the simplified model structure fibers are in an orderly arrangement whereby fibers in a plane lie parallel to each other but perpendicular to fibers in adjacent planes (Fig. 9). For CBCF, making the assumptions of isotropic fibers, fiber emissivity of 1 and matrix making no contribution to thermal conductivity, expressions for solid, radiation and gas heat transfer, shown in Table II, have been derived from the work of Donaldson [10], Larson and Churchill [26] and Hager and Sterre [27], respectively, as described in reference 11. In the equations ρ is the density of CBCF, ρ_f is the density of the fibers (1.4 Mgm^{-3}), d is the diameter of the fibers, σ is Stefan-Boltzman constant, and k_f and k_g are the thermal conductivity of the fiber and gas, respectively. Thermal conductivity perpendicular to the fiber array (z-direction) at 1000°C, 1600°C and 2200°C for unpurified CBCF heat treated at 2200°C are calculated and compared against the experimental results that are also presented in Table II. The thermal conductivity values for carbon fibers and argon are taken from references 31 and 32, respectively. From the table it can be seen that the model does offer reasonable agreement with the experimental values especially considering the simplifications regarding the fiber arrangement and the uncertainty in the values used for the fiber thermal

TABLE II Thermal conductivity perpendicular to the fiber array (z-direction) calculated using a model and compared with experimental values for unpurified CBCF heat treated at 2200°C

Temperature (°C)	Solid conduction ($Wm^{-1}K^{-1}$) $= \frac{6.5\rho^2 k_f}{1+3.6\rho}$	Radiation conduction ($Wm^{-1}K^{-1}$) $= 5\sigma T^3 \frac{d\rho_f}{\rho}$	Gas conduction ($Wm^{-1}K^{-1}$) $= \frac{k_g k_f \rho_f}{k_f(\rho_f-\rho)+k_g\rho}$	Theoretical thermal conductivity ($Wm^{-1}K^{-1}$)	Experimental thermal conductivity ($Wm^{-1}K^{-1}$)
1000	0.38 (79%)	0.05 (9%)	0.06 (12%)	0.49	0.39
1600	0.47 (69%)	0.15 (21%)	0.07 (10%)	0.69	0.55
2200	0.73 (63%)	0.33 (29%)	0.09 (8%)	1.15	0.84

conductivity. The model suggests that at all temperatures solid heat transfer is the major contributor to the overall conductivity; however, the contribution does decrease from 79% to 63% as the test temperature increased from 1000°C to 2200°C. On the other hand according to the model the radiation contribution increases with test temperature and accounts for 29% of the total thermal conductivity at 2200°C.

The dominance of the solid thermal conductivity contribution suggested by the model is consistent with the increase in thermal conductivity of CBCF as the temperature is increased. In the case of solid thermal conductivity dominance, the thermal behavior of CBCF is determined by the intrinsic behavior of the relatively amorphous fibers. An increase of thermal conductivity with temperature is typical of non-graphitic carbons for which, due to their small crystallite size, the phonon mean free path is determined by phonon-defect interaction [33]. The non-graphitizing nature of fibers, indicated by the Raman results, is confirmed by the fact that for CBCF the thermal conductivity increases with temperature even for the sample heat treated at 3000°C.

One possible explanation for why heat treatment results in a relatively large increase in the thermal conductivity in the x-direction compared to that in the z-direction is that the axial thermal conductivity of the fibers is increased but a relatively small change occurs in the transverse fiber thermal conductivity. However, the fibers show no optical anisotropy even after heat treatment at 3000°C indicating a low extent of preferred orientation. In addition, Raman examination indicated that heat treatment resulted in relatively little structural change in the case of the fibers. These observations indicate that it is unlikely that heat treatment even at 3000°C results in fibers with highly anisotropic thermal conductivity properties.

An alternative explanation is that there is an increase in effective axial thermal conductivity of the fiber due to a contribution by the coating of matrix noted in the optical microscopy investigation. Although the matrix only accounts for 10% of the mass of the composite and the coating of matrix on the fiber is not continuous the large transformation towards graphite and the likely orientation of the graphite planes parallel with the fiber surface may contribute to the thermal conductivity in the axial direction of the fiber. Considering that the Raman parameters of the matrix heat treated at 3000°C are similar to those of HOPG the thermal conductivity of the matrix may approach that of HOPG. The thermal conductivity of HOPG, parallel with the graphite planes, is 400 $Wm^{-1}K^{-1}$ at 1000°C which is more than two orders of magnitude greater than that of the fiber which is 3 $Wm^{-1}K^{-1}$ at the same temperature [34]. As shown by Donaldson, for CBCF containing fibers with anisotropic thermal conductivity properties the thermal conductivity in the z-direction is largely determined by the lower transverse conductivity of the fibers [10]. Evidently, if the coating of matrix completely surrounded the fiber an increase in the effective transverse fiber thermal conductivity would result. However, from optical microscopy matrix is usually observed in the grooves of the fiber's crenellated cross-section and generally does not completely surround the fiber (for example see top right of Fig. 3a). A complete coating around the circumference of the fiber is inhibited by the fiber's crenellated cross-section that encourages the melted resin to flow axially down the grooves as opposed to circumferencially. Therefore, it is reasonable to suggest that the matrix may contribute to the effective axial thermal conductivity of the fiber and have relatively little effect on the transverse thermal conductivity. The increase in effective axial thermal conductivity of the fiber due to matrix contribution is consistent with the relatively large increase in thermal conductivity of CBCF in x-direction compared to that in the z-direction after heat treatment.

Models of thermal conductivity behavior of CBCF assume that the matrix does not make any contribution to the thermal conductivity. This assumption was made because the structure of the matrix was thought to be non-graphitic and the matrix concentrated at the fiber junctions. However, we have shown here that the matrix has a more graphitic-like structure compared to the fibers, and hence a greater thermal conductivity, and is present to a certain extent along the length of the fibers. However, although the matrix may make a contribution, especially parallel with the fiber array (x-direction), the thermal conductivity of CBCF is still determined by the non-graphitic fibers as even after heat treatment at 3000°C the thermal conductivity, in both directions, is found to increase with test temperature, a behavior typical of non-graphitic carbons.

4. Conclusion

Halogen purification was found not to effect the structure of CBCF to a greater extent than heat treatment at the same temperature in inert atmosphere. Optical microscopy of both halogen purified and unpurified CBCF showed that the matrix was anisotropic where

as the fibers were optically isotropic. Raman spectroscopy was used to show that the matrix was more graphitic in nature compared to the fibers and underwent a greater structural change on heat treatment. The thermal conductivity of all specimens was found to increase with temperature, typical of non-graphitic carbons. Heat treatment resulted in a large increase in the thermal conductivity parallel to the fiber array compared to the perpendicular direction. Although models of the thermal conductivity of CBCF assumed that the matrix was not significant the highly graphitic nature of matrix present in the grooves of the crenellated carbon fibers may contribute to the increase in the thermal conductivity in the direction parallel to the fiber array.

Acknowledgements

Dr. Baxter is grateful to the Science and Technology Agency for supporting him as a Science and Technology Agency research fellow. The authors wish to express to Chris Gee and Steve Ellacott of Calcarb Ltd (12 North Road, Bellshill, Strathclyde, ML4 1EN) for their assistance in providing materials for this work.

References

1. G. C. WEI and J. M. ROBBINS, *Amer. Ceram. Bull.* **64** (1985) 691.
2. I. J. DAVIES and R. D. RAWLINGS, *J. Mater. Sci.* **29** (1994) 338.
3. R. I. BAXTER and R. D. RAWLINGS, *Mater. Sci. and Technol.* **4** (1998) 161.
4. I. J. DAVIES and R. D. RAWLINGS, *Composites* **25** (1994) 229.
5. *Idem.*, *Carbon* **32** (1994) 1449.
6. S. D. ELLACOTT, M.Sc. thesis, University of Surrey, Guildford, UK, 1994.
7. I. J. DAVIES and R. D. RAWLINGS, *Compos. Sci. Technol.* **59** (1999) 97.
8. R. I. BAXTER and R. D. RAWLINGS, *J. Mater. Sci.* **32** (1997) 4485.
9. T. G. GODFREY, D. L. MCELROY and Z. L. ARDARY, *Nuclear Technol.* **22** (1974) 94.
10. A. B. DONALDSON, in Proceedings of Heat Transfer Conference, Atlanta, August 1973, paper 73-HT-44.
11. R. I. BAXTER, R. D. RAWLINGS, N. IWASHITA and Y. SAWADA, accepted to Carbon, Dec. 1998.
12. DEGASSA company information sheet, Germany, February 1989.
13. R. I. BAXTER, PhD thesis, University of London, 1996.
14. T. NODA and M. INAGAKI, *Carbon* **2** (1964) 127.
15. T. SUZUKI and K. KANEKO, *ibid.* **26** (1988) 743.
16. P. M. ADAMS, H. A. KATZMAN, G. S. RELLICK and G. W. STUPIAN, *ibid.* **26** (1998) 233.
17. ASTM Designation E1461-92.
18. R. E. TAYLOR, *High temperatures-High pressures* **11** (1979) 43.
19. R. D. COWAN, *J. Appl. Phys.* **34** (1963) 926.
20. CALCARB company internal report, Scotland, September 1990.
21. B. D. CULLITY, "Elements of x-ray diffraction" 2nd ed. (Addison-Wesley Co., USA, 1978) p. 87, 102.
22. K. AGONI, *Carbon* **31** (1993) 537.
23. E. FITZER and L. M. MANOCHA, "Carbon reinforced and carbon/carbon composites" (Springer-Verlag, Germany, 1998) p. 166.
24. G. M. JENKINS and K. KAWAMURA, "Polymeric carbons, carbon fiber, glass and char" (Cambridge University Press, UK, 1976).
25. M. A. SHORT and P. L. WALKER, *Carbon* **1** (1963) 3.
26. B. K. LARKIN and S. W. CHURCHILL, *AIChE Journal* **5** (1959) 467.
27. N. E. HAGER and R. C. STEERE, *J. Appl. Phys.* **38** (1967) 4633.
28. M. S. DRESSELHAUS, G. DRESSELHAUS, K. SUGIHARA, I. L. SPAIN and H. A. GOLDBERG, "Graphite fibers and filaments" (Springer-Verlag, Berlin, 1988) p. 98.
29. F. TUINSTRA and J. L. KOENIG, *J. Compos. Mater.* **4** (1970) 492.
30. T. C. CHIEU, M. S. DRESSELHAUS and M. ENDO, *Physical Review B* **26** (1982) 5867.
31. C. Y. HO, R. W. POWELL and P. E. LILEY, *J. Physical and Chemical reference data* **1** (1972) 317.
32. *Idem.*, *ibid.* **1** (1972) 308.
33. G. SAVAGE, "Carbon-carbon composites" (Chapman and Hall, London, 1993) p. 311.
34. C. Y. HO, R. W. POWELL and P. E. LILEY, *J. Physical and Chemical reference data* **1** (1972) 323.

Received 14 April
and accepted 19 May 1999